

Laboratory Observation of Ion Conics by Velocity-Space Tomography of a Plasma

R. McWilliams and R. Koslover

Department of Physics, University of California, Irvine, California 92717

(Received 17 March 1986)

Laboratory experiments have examined particular elements of proposed mechanisms for ion conic formation seen in the Earth's auroral-zone magnetosphere. A laser-induced fluorescence diagnostic measured the ion distribution function at many angles in velocity space, allowing tomographic techniques to reconstruct the multidimensional ion distribution function. Ion conics, as well as drifting Maxwellians, were observed.

PACS numbers: 52.70.Kz, 52.35.Fp, 52.70.Nc, 94.30.Gm

Ion conics are observed in the Earth's auroral-zone magnetosphere through the use of ion-energy analyzers on satellites.¹ These conical distributions in velocity space are seen in conjunction with double layers,^{2,3} electrostatic ion-cyclotron waves,^{4,5} and lower hybrid waves.^{6,7} One suggested mechanism of ion conic formation is perpendicular (to the geomagnetic field) ion heating due to waves, followed by $\mu\nabla B$ forces folding the distribution into a conic. Laboratory experiments at the University of California, Irvine, are simulating aspects of the magnetosphere to examine the processes which may be responsible for the satellite data. In this Letter we report observations of drifting undisturbed Maxwellian velocity distributions and the first laboratory observations of ion conic production in the presence of radio frequency waves. These measurements were made by a new technique of optical tomography⁸ in velocity space.

Previously, a direct measure of multidimensional ion-velocity distribution functions was difficult to achieve. Typically, laboratory ion-energy analyzers have a wide particle-acceptance angle and therefore good angular resolution is difficult to obtain. Also, the distribution function usually can be inferred only by the taking of the derivative of a signal, a risky process. Lastly, the presence of an energy analyzer in a laboratory plasma may be a significant perturbation to the system. With these difficulties in mind, experiments can still benefit substantially from analyzer data, both in space¹ and in the laboratory.⁹

Laser-induced fluorescence¹⁰⁻¹⁴ has been used in the laboratory to measure one-dimensional ion distribution functions. A single-frequency (ω_L) laser beam characterized by a wave vector \mathbf{k}_L is sent through a plasma. Ions at velocity \mathbf{v}_i having an electronic transition frequency ω_0 may undergo a transition and emit a photon upon relaxing to another state when the required Doppler shift

$$\omega_L - \mathbf{k}_L \cdot \mathbf{v}_i = \omega_0 \quad (1)$$

is satisfied. The emitted photon flux is proportional to the number density of ions satisfying Eq. (1). Scanning of the laser frequency can then yield the complete one-

dimensional velocity distribution function. The one-dimensional nature of the distribution function is arrived at because of the scalar product in Eq. (1) which, in essence, means that the measuring technique integrates over the two dimensions perpendicular to \mathbf{k}_L , e.g.,

$$f_i(\mathbf{x}, v_x, t) = \int f_i(\mathbf{x}, \mathbf{v}, t) dv_y dv_z. \quad (2)$$

It is important to note that this method of measuring ion distributions is nonperturbing to the plasma, has good spatial resolution (1 mm³) and good speed resolution (3×10^3 cm/s or about $3 \times 10^{-2} v_{ti}$ for this experiment), and does not require substantial inference.

Having obtained a one-dimensional distribution, one may now expand to two and three dimensions by the use of a new technique we shall call optical tomography⁸ in velocity space. At constant position \mathbf{x} , one may take a set of distributions (typically distributed uniformly in two or three dimensions), at arbitrary angles, Ψ_L , by causing \mathbf{k}_L to change direction when the laser beam is rotated through the angles of interest (see Fig. 1). Given the difficulty of presentation of four-dimensional plots, we will use only two velocity dimensions in this Letter. Having a set of scans at different angles in velocity space

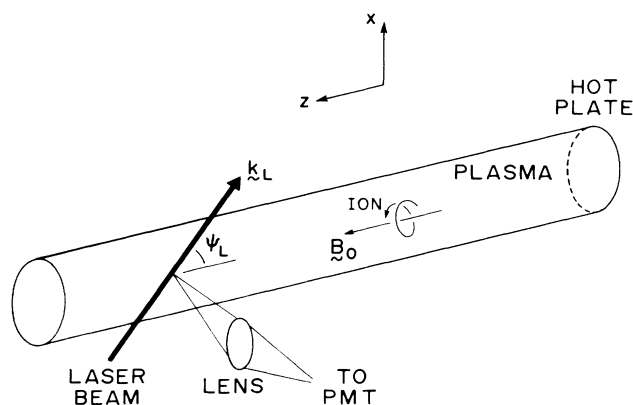


FIG. 1. Schematic of experimental arrangement showing cylindrical plasma, coordinate system, and laser beam at angle Ψ_L in the x - z plane.

permits the use of tomographic methods by the use of the Radon transform¹⁵ and filtered back projection.¹⁶ A more detailed description of the equipment and techniques may be obtained in Ref. 8.

The magnetospheric simulation experiments reported here were performed in a single-ended *Q* machine¹⁷ (see Fig. 1) which provided a low-density ($n \approx 10^{10} \text{ cm}^{-3}$), low-temperature ($T_i \approx T_e \approx 0.2 \text{ eV}$), nearly completely ionized barium plasma 1.0 m long and 5 cm in diameter. The confining magnetic field was 6 kG.

An undisturbed plasma formed at the hot plate will drift axially to the opposite end of the machine where it is lost. One might expect the ion distribution function to be approximately a drifting Maxwellian. A set of laser scans at many (8–16) angles in the *x-z* plane was taken and unfolded to give $f_i(\mathbf{x}, v_x, v_z, t)$. As discussed in Ref. 8, the angles Ψ_L are uniformly distributed in the *x-z* plane for $0 \leq \Psi_L \leq \pi$ (the information for $\pi \leq \Psi_L \leq 2\pi$ is in this set since the laser scan samples negative through positive velocities at every Ψ_L). Generally, the more angles in a set, the greater the resolution. It should be noted that no particular component of \mathbf{v} is favored by this sampling technique. Kinetic effects have been discussed by Stern¹⁸ and Hill, Fornaca, and Wickham¹⁴

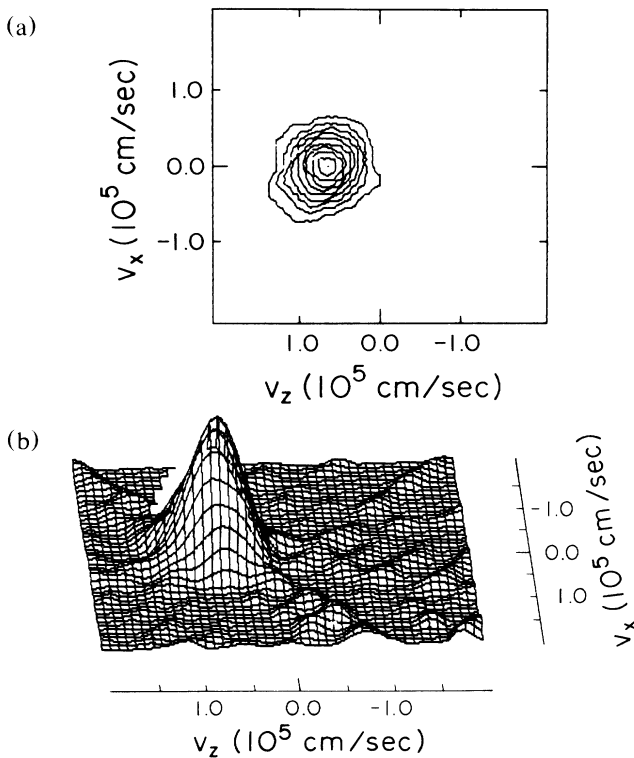


FIG. 2. Ion distribution function of undisturbed, drifting nearly Maxwellian plasma. (a) Contours of constant f_i in 10% increments. (b) Perspective drawing with f_i proportional to the distance of the plotted point from the v_x - v_z plane.

and are considered here. In Fig. 2, two ways to view $f_i(\mathbf{x}, v_x, v_z, t)$ are displayed. Ten sampling angles were used to obtain this graph. Figure 2(a) shows the two-dimensional ion distribution function plotted by use of contours running along lines of constant f_i in the plot. The plasma has an axial drift down the magnetic field of about $6.4 \times 10^4 \text{ cm/s}$. The perpendicular ion temperature is about 0.17 eV with the parallel ion temperature of 0.15 eV. The drift speed, $T_{i\perp}$, and $T_{i\parallel}$ are consistent with plasma-sheath acceleration effects in front of the hot plate. Integrated one-dimensional distribution functions have shown previously the parallel and perpendicular components¹⁴ of this measurement, but have not shown multidimensional distribution functions. Figure 2(b) shows a plot of the distribution function with the distance of the plotted point out of the v_x - v_z plane proportional to f_i . The low-level ripples running from the center of the distribution to the edges of the graph are artifacts of the reconstruction technique which become decreasingly visible as the number of angles scanned increases. The drifting Maxwellian nature is seen easily in Fig. 2(b) while Fig. 2(a) shows some detail better. While the diagnostic can resolve $2 \mu\text{s}$ temporally, the data presented are time-average distributions for comparison with satellite data.¹

An electrostatic ion-cyclotron instability^{19,20} was produced^{21,22} by our drawing an axial electron current to a biased button in a 6-mm channel down the axis of the machine. Such a configuration creates electron flow and dc potential profiles²³ (see Fig. 3, provided by Lang²⁴) similar in shape to those observed in the magnetosphere.²

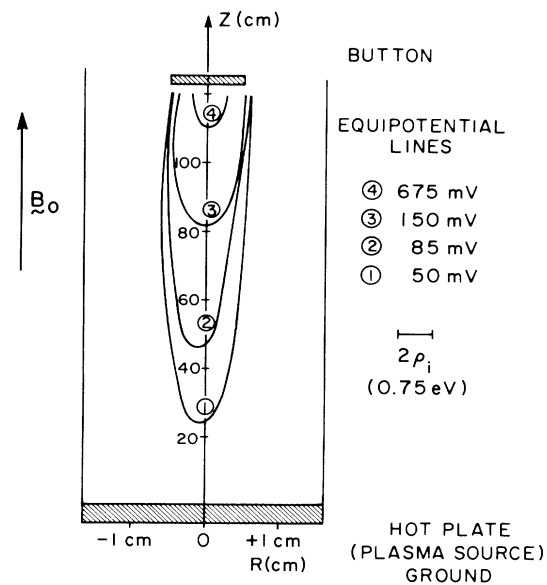


FIG. 3. Contours of constant potential obtained when a very large-amplitude electrostatic ion-cyclotron wave is driven by an electron current drawn to the button. Figure provided by Lang, Ref. 24.

Note that the experiment has a linear magnetic field while the Earth's lower magnetosphere has the flaring field lines of a dipole. Several experiments^{13,14,23,25,26} have used laser-induced fluorescence to diagnose particulars of this instability such as density fluctuations, but none have reported multidimensional distribution measurements and hence such structures as ion conics have not been observed previously. A recent paper²⁷ discusses ion-energy-analyzer measurements of parallel and perpendicular heating for a similar experiment in a flaring magnetic field configuration. When large-amplitude waves, $e\phi/T \geq 1$, were excited, substantial changes in the distribution function occurred, as shown in Fig. 4 (sixteen sampling angles were used to obtain this graph). An ion conic may be characterized as a distribution function where the contours of constant f_i form a conical shape in velocity space, rather than the circular shapes of Fig. 2, commonly having the vertex near $\mathbf{v}=0$ and axis of the cone along the v_z axis. In Fig. 4 one sees an ion conic distribution quite similar in shape to magnetospheric observations.¹ The conic nature is discernible up through the fortieth percentile contour while the instrumental and reconstruction resolution is about 4% here. The location of the tomographic measurement was radially at the current-channel center and axially at about the equivalent Fig. 3 position of $z=80$ cm. The ion distribution function is stretched in the perpendicular direction as ions are heated by the instability in their transit down the machine. We speculate that the ion conic is formed as a result of the heated distribution interacting with the dc potential structure. To see this, consider two ions with the same v_{\parallel} and different v_{\perp} values. The ions must suffer a deceleration to reach the measurement location. The ion with the larger pitch angle will give up less δv_{\parallel} in doing work against the dc electric field than the smaller-pitch-angle ion to reach the measurement position (note also that their paths to this position are

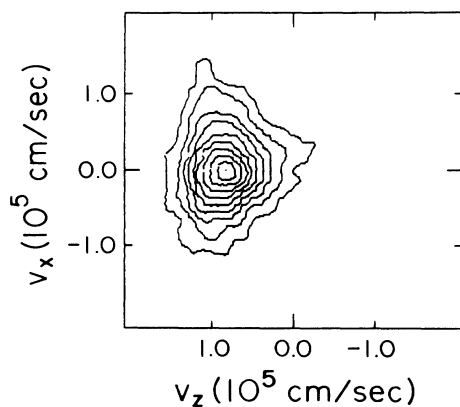


FIG. 4. Ion distribution function showing ion conic formed by production of a large-amplitude electrostatic ion-cyclotron instability in a plasma which was characterized by Fig. 2 before driving of the instability.

not identical). Hence, a perpendicularly heated ion distribution interacting with such a potential structure could form an ion conic.

Lower hybrid waves have been proposed⁷ as a mechanism for perpendicular ion heating in the auroral magnetosphere. In fact, perpendicular ion heating from waves generated near ω_{pi} was a suggested energy channel for the electron-slideaway-regime operation of the Alcator tokamak.²⁸ Additionally, ion-energy-analyzer measurements showed increases in perpendicular ion temperature when the cross-field-current driven lower hybrid instability was driven by an electron current.²⁹

In the laboratory, lower hybrid waves were launched from a 12-cm axial extent cylindrical antenna³⁰ which was coaxial with the plasma column. The waves were broad band in frequency with the center frequency about twice the ion plasma frequency. The waves were detected throughout the plasma by means of small, radially moveable coaxial rf probes with 3-mm tips oriented along the magnetic field lines. We have reported a study of such wave effects on perpendicular distributions.³¹

Figure 5 shows the ion response to large-amplitude ($e\phi/T \geq 1$) lower hybrid waves launched from the antenna. Eight sampling angles were used in this figure, yielding resolution of only (8-10)%, which shows mostly in the incoherent structure of the lowest-level contour. Substantial heating is seen in the perpendicular direction while the parallel ion distribution remains nearly unchanged as is expected for $k \approx k_{\perp}$ in the waves. For the figure $T_{i\perp}/T_{i\parallel} = 2.1$. There is only a hint of an ion conic, but it is not substantial, and is at the level of resolution for this figure which is consistent with the conic of Fig. 4 being produced by heating plus the potential structure (not found for the lower hybrid experiment). Up to a factor of 6 increase in $T_{i\perp}$ has been observed with less than a 25% change in $T_{i\parallel}$. Clearly, the next step would be to perform these experiments in a dipole magnetic

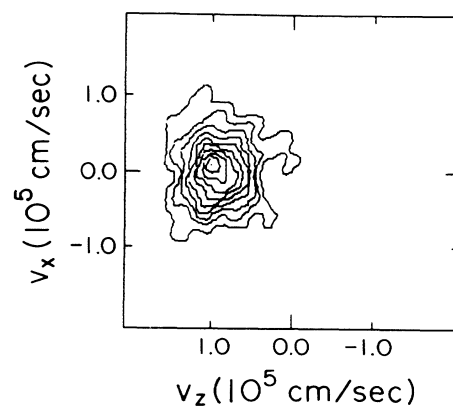


FIG. 5. Ion distribution function when large-amplitude, broad-band lower hybrid waves are launched into a plasma initially characterized by Fig. 2. Note substantial perpendicular heating.

field geometry, where $\mu\nabla B$ forces might produce a conic.

In summary, a direct, nonperturbing optical tomography diagnostic has been developed which measures multidimensional ion velocity-space distribution functions. In laboratory experiments, large-amplitude waves can modify a drifting Maxwellian plasma to form ion conic distributions similar to those observed by satellite measurements.

The authors thank Dr. Nathan Rynn for discussions and Mr. Mason Okubo and Mr. Stacy Roe for technical assistance. This work was supported by National Science Foundation Grants No. ATM84-11189 and No. PHY-8306108.

¹R. D. Sharp, R. G. Johnson, and E. G. Shelley, *J. Geophys. Res.* **82**, 3324 (1977); P. F. Mizera *et al.*, *J. Geophys. Res.* **86**, 2329 (1981); D. J. Gorney, *Adv. Space Res.* **4**, 499 (1984).

²F. S. Mozer, *et al.*, *Phys. Rev. Lett.* **38**, 292 (1977).

³J. E. Borovsky, *J. Geophys. Res.* **89**, 2251 (1984).

⁴P. M. Kintner, M. C. Kelley, and F. S. Mozer, *Geophys. Res. Lett.* **5**, 139 (1978).

⁵M. Ashour-Abdalla, H. Okuda, and C. Z. Cheng, *Geophys. Res. Lett.* **8**, 795 (1981).

⁶F. S. Mozer *et al.*, *J. Geophys. Res.* **84**, 5875 (1979).

⁷T. Chang and B. Coppi, *Geophys. Res. Lett.* **8**, 1253 (1981).

⁸R. Koslover and R. McWilliams, *Rev. Sci. Instrum.* **57**, 2441 (1986).

⁹R. L. Stenzel, W. Gekelman, and N. Wild, *Phys. Fluids* **26**, 1949 (1983).

¹⁰R. M. Measures, *J. Appl. Phys.* **39**, 5232 (1968).

¹¹D. Dimock, E. Hinnov, and L. C. Johnson, *Phys. Fluids* **12**, 1730 (1969).

¹²R. A. Stern and J. A. Johnson, *Phys. Rev. Lett.* **34**, 1548 (1975).

¹³R. A. Stern, D. N. Hill, and N. Rynn, *Phys. Rev. Lett.* **47**,

792 (1981).

¹⁴D. N. Hill, S. Fornaca, and M. G. Wickham, *Rev. Sci. Instrum.* **54**, 309 (1983).

¹⁵J. Radon, *Math. Phys. Kl.* **69**, 262 (1917).

¹⁶R. N. Bracewell and A. C. Riddle, *Astrophys. J.* **150**, 427 (1967).

¹⁷N. Rynn, *Rev. Sci. Instrum.* **35**, 40 (1964).

¹⁸R. A. Stern, *Phys. Fluids* **21**, 1287 (1978).

¹⁹W. E. Drummond and M. N. Rosenbluth, *Phys. Fluids* **5**, 1507 (1962).

²⁰J. M. Kindel and C. F. Kennel, *J. Geophys. Res.* **76**, 3055 (1971).

²¹N. D'Angelo and R. W. Motley, *Phys. Fluids* **5**, 633 (1962).

²²N. Rynn, D. R. Dakin, D. L. Correll, and G. Benford, *Phys. Rev. Lett.* **33**, 765 (1974).

²³A. Lang and H. Boehmer, *J. Geophys. Res.* **88**, 5564 (1983).

²⁴H. Boehmer and A. Lang, in *Physics of Auroral Arc Formation*, edited by S. I. Akasofu and J. R. Kan, Geophysical Monograph Series Vol. 25 (American Geophysical Institute, Alexandria, VA, 1981), p. 380; Ph.D. thesis, University of California, Irvine, 1984 (unpublished).

²⁵R. A. Stern, D. L. Correll, H. Boehmer, and N. Rynn, *Phys. Rev. Lett.* **37**, 833 (1976).

²⁶R. A. Stern, D. N. Hill, and N. Rynn, *Phys. Lett.* **93A**, 127 (1983).

²⁷S. L. Cartier, N. D'Angelo, and R. L. Merlino, *J. Geophys. Res.* **91**, 8025 (1986).

²⁸B. Coppi, F. Pegoraro, R. Pozzoli, and G. Rewoldt, *Nucl. Fusion* **16**, 309 (1976).

²⁹M. Yamada and D. K. Owens, *Phys. Rev. Lett.* **38**, 1529 (1977).

³⁰P. Bellan and M. Porkolab, *Phys. Rev. Lett.* **34**, 124 (1975).

³¹R. McWilliams, R. Koslover, H. Boehmer, and N. Rynn, in *Ion Acceleration in the Magnetosphere and Ionosphere* (American Geophysical Union, Washington, DC, 1986), p. 245.